Effects of Clay Dispersion on the Foam Morphology of LDPE/Clay Nanocomposites

Y. H. Lee,[1] K. H. Wang,[2] C. B. Park,[2] M. Sain[1]

[1]*Faculty of Forestry, Center for Biocomposites and Biomaterials Processing, University of Toronto, Toronto, Ontario, Canada M5S 3B3*
[2]*Department of Mechanical and Industrial Engineering, Microcellular Plastics Manufacturing Laboratory, University of Toronto, Toronto, Ontario, Canada M5S 3G8*

Received 7 June 2005; accepted 6 June 2006
DOI 10.1002/app.24908
Published online in Wiley InterScience (www.interscience.wiley.com).

ABSTRACT: Intercalated and exfoliated low-density polyethylene (LDPE)/clay nanocomposites were prepared by melt blending with and without a maleated polyethylene (PE-g-MAn) as the coupling agent. Their morphology was examined and confirmed by X-ray diffraction (XRD) and transmission electron microscopy (TEM). The effects of clay content and dispersion on the cell morphology of nanocomposite foams during extrusion foaming process were also thoroughly investigated, especially with a small amount of clay of 0.05–1.0 wt%. This research shows the optimum clay content for achieving microcellular PE/clay nanocomposite foams blown with supercritical CO_2. It is found that < 0.1 wt% of clay addition can produce the microcellular foam structure with a cell density of $> 10^9$ cells/cm^3 and a cell size of ~ 5 μm. © 2006 Wiley Periodicals, Inc. J Appl Polym Sci 103: 2129–2134, 2007

Key words: nanocomposites; LDPE; foam; clay; microcellular

INTRODUCTION

Considerable effort has been devoted to the development of foams characterized by morphologies that demonstrate reduced cell sizes and narrower cell size distribution for many applications, such as electronic and automobile materials, due to improved mechanical properties.[1–5] Microcellular plastics are polymer foams with an average cell size of < 10 μm and cell density of $> 10^9$ cells/cm^3. Compared with unfoamed polymers, the unique structure of microcellular foamed plastics offers superior relative mechanical properties in terms of their impact strength, toughness, and fatigue life.[1–5]

Recently, extensive research has been conducted in the area of microcellular foaming while using various thermoplastic materials. However, there have been very few studies that report microcellular foaming of polyolefin-based materials in extrusion. This is due to the inherently poor cell nucleation behavior of polyolefins.[6–8] To overcome this difficulty, Park and colleagues.[9–11] explored the idea of using a higher amount of supercritical CO_2 and a nucleating agent and/or using polymer blending, and cross-linking to get microcellular low-density polyethylene (LDPE) foams. Their results showed that the cell density was improved significantly. In this context, several researchers have studied the influence of the nucleating agent on cell morphology, such as foam cell size, distribution, and density. Lee et al.[12] examined the gas absorption behavior of polymer systems [high-density polyethylene (HDPE) with/without talc, and PVC with/without $CaCO_3$] to explain heterogeneous nucleation in mineral-filled polymers. It was suggested that the accumulated gas in the filler–polymer interface helps to create cells in the foaming process. Ramesh et al.[13,14] developed a model for heterogeneous nucleation based on the presence of microvoids in polystyrene (PS) and high-impact polystyrene (HIPS) blends.

During the past decade, the use of layered silicate nanoparticles, i.e., clay to reinforce polymers has drawn a great deal of attention. Polymer nanocomposites consist of a polymer matrix, filled with layered silicates that are dispersed at a nanoscale level. Adding a small amount of clay (~ 5 wt %) can dramatically improve a wide variety of properties of the polymer matrix.[15–18] Interest in polyolefin nanocomposites in particular has emerged due to the fact that they promise enhanced performance in packaging and automobile applications. Chemical modification of polyolefins, especially via the grafting of the pendant anhydride group, have been used success-

Correspondence to: C. B. Park (park@mie.utoronto.ca).
Contract grant sponsor: Consortium for Cellular and Microcellular Plastics (CCMCP).
Contract grant sponsor: Natural Science and Engineering Research Council of Canada (NSERC).

fully to overcome problems associated with poor interfacial interaction as a coupling agent in polyolefin/clay systems.[19–21] Intercalated and/or exfoliated structures can be generated, depending on the amount of added coupling agent, the compounding method, and the processing conditions, resulting in a corresponding increase in mechanical properties due to improved interfacial adhesion.

In comparison with conventional micron-sized filler particles used in foaming processes, nanometer-sized clay particles may offer unique properties. The large surface area of exfoliated clay nanoparticles with their extremely fine dimensions (high aspect ratios of > 200), and intimate contact between particles and polymer matrix may greatly alter the cell nucleation and growth behaviors. Therefore, it would be most beneficial to discover how the nanoparticles affect the foaming behavior. Lee and coworkers[22,23] demonstrated that the addition of small amount of clay (5 wt %) could reduce cell size and increase cell density in PS/clay nanocomposites foams by using CO_2 in both extrusion foaming process and batch process. These investigators also investigated the combined effect of nanoclay and CO_2 on polymer melt rheology for an extrusion process.[24] Without the presence of CO_2, the viscosity of the nanocomposite increase with nanoclay loading. However, when the nanocomposite melt is swollen by CO_2, the nanoclay acts to reduce viscosity when compared with the pure PS/ CO_2 system. Okamoto and coworkers[25] studied the influence of clay particles (2–7.5 wt %) on the cell density, cell size, cell wall thickness and bulk density for foamed maleated polypropylene/clay nanocomposites. TEM observation showed that biaxial flow during cell growth induces the alignment of clay particles along the cell boundary. These investigators also conducted foam processing on polylactide (PLA)/clay (3.5 wt %) nanocomposites via batch process in an autoclave by using supercritical CO_2 as a foaming agent.[26] The morphological correlation between the dispersed clay particles with nanometer dimensions in bulk and the closed-cell structure of the foam was examined. Turng and colleagues[27] explored the processing benefits and property improvements of combined nanocomposites with microcellular injection molding. Compared with the corresponding base polyamide microcellular parts, the microcellular nanocomposites exhibited better cell structures and cell distributions, as well as better mechanical properties.

This research investigates the effects of the degree of clay exfoliation on the cell morphology of LDPE/clay nanocomposites, especially those that contain only a very small amount of clay (in the range of 0.05–1.0 wt %). Also, the optimum content of clay to get microcellular LDPE nanocomposite foams was explored.

EXPERIMENTAL

Materials

In this study, LDPE (LA-0124, NOVA Chemicals, Calgary, Alberta, Canada), with a density of 0.924 g/cm^3 and a melt index of 1.5 g/10 min, was used. Organically modified clay with dimethyl dehydrogenated tallow alkyl ammonium (Cloisite 20A, Southern Clay Products, Austin, TX) was employed as a layered silicate. LLDPE-g-maleic anhydride (PE-g-MAn, Fusabond MB226D, $\sim$ 1.0 wt % of maleic anhydride, MI 1.5 g/10 min, DuPont Canada, Kingston, Ontario, Canada) was used as a coupling agent. A commercial-grade carbon dioxide (purity: 99.5%, BOC Gas Products, Mississauga, Ontario, Canada) was used as a blowing agent without any further purification.

Preparation and characterization of LDPE/clay nanocomposites

LDPE/clay nanocomposites were prepared using a 30 mmΦ intermeshing twin screw extruder (W&P ZSK30, 40 : 1 L/D) operated in a co-rotating mode. The screw rotating speed was 250 rpm and the extrusion temperature was 150 °C. For nanocomposites containing a coupling agent, the clay contents were varied across a range of 0.02–5.0 wt %, and PE-g-MAn content was fixed at 15 wt %; these nanocomposites were correspondingly denoted as WC0.02–WC5.0. Nanocomposites without a coupling agent were also prepared by adding different amounts of clay (0.05, 0.5 wt %) with pure LDPE, and were denoted as NC0.05 and NC0.5, respectively; 0.02–1.0 wt % of the clay was compounded into pure LDPE with a concentrate of 5.0 wt %, which were further diluted with additional pure LDPE to obtain the designated clay levels.

The nanocomposite structure was characterized by wide-angle X-ray diffraction (XRD) and transmission electron microscopy (TEM). XRD was conducted using a Siemens D5000 diffractometer using Cu Kα radiation (1.548 Å) with a Kevex solid-state detector. Measurement was performed at 50 kV and 35 mA. The data were recorded in the reflection mode in the range of $2\theta = 1.5$–10°, using STEP scan mode; the step size was 0.02°, and the counting time was 2.0 s per step. For the TEM analysis, the specimen was microtomed to an ultrathin section of 70-nm thickness, using an ultra-cryomicrotome with a diamond knife. The structure was observed by using a FEI Technai 20 (Phillips, Hillsboro, OR) microscope at 100 kV.

Preparation and characterization of LDPE/clay nanocomposite foams

The cellular foamability of these nanocomposites was studied by using a physical blowing agent

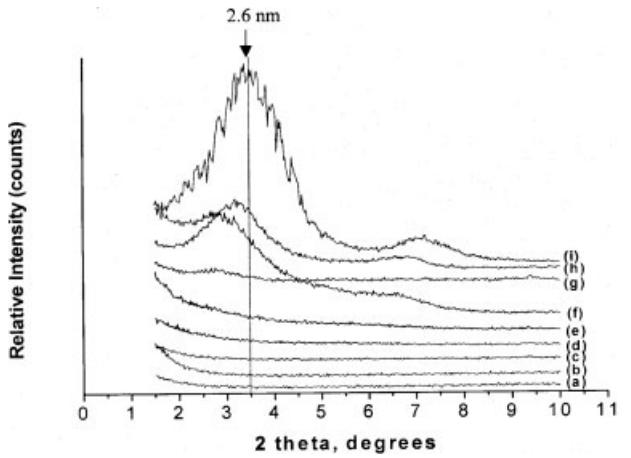

Figure 1 X-ray diffraction patterns for LDPE/clay nanocomposites with increasing clay content (a) WC0.02, (b) WC0.05, (c) WC0.1, (d) WC0.5, (e) WC1.0, (f) WC5.0, (g) NC0.05, (h) NC0.5, (i) pure clay.

(PBA), CO_2 (8 wt %) through single extrusion process. The die temperature was varied from 110°C to 90°C with a decrement of 5°C. The collected foam samples were chosen at random, and the morphological dimensions, such as the cell size and cell density, were examined by scanning electron microscopy (SEM, Hitachi S-2500). The volume expansion ratio of each sample was calculated as the ratio of the density of the original sample (ρ_0) to the measured density of the foam sample (ρ_f). The cell density (N_f) was estimated by eq. (1), in which the area of the micrograph was A cm^2, the number of bubbles, n, and the magnification factor was M:

$$N_f = \left(\frac{nM^2}{A}\right)^{3/2} \times \frac{\rho_o}{\rho_f}. \quad (1)$$

RESULTS AND DISCUSSION

Structure of LDPE/clay nanocomposites

The structure of nanocomposites has been elucidated using XRD and TEM. Figure 1 shows the XRD patterns of LDPE/clay nanocomposites used in this study. There were no clay characteristic peaks for the LDPE nanocomposites that were filled with clay amounts ranging from 0.02 to 1.0 wt % with PE-g-MAn [WC0.02 (a) to WC1.0 (e)], suggesting that most of the clay particles exists in the exfoliated state in the LDPE matrix. These features can be seen clearly in the TEM images of WC0.05 and WC0.5 samples, shown in Figure 2, which shows uniform dispersion of the delaminated clay particles in the LDPE matrix. However, the WC5.0 (f) shows a strong diffraction peak at a lower angle than that of pure clay, signaling that an intercalated nanocomposite was formed. It is apparent therefore that at constant processing conditions, clay concentration affects the exfoliation. According to the delamination/

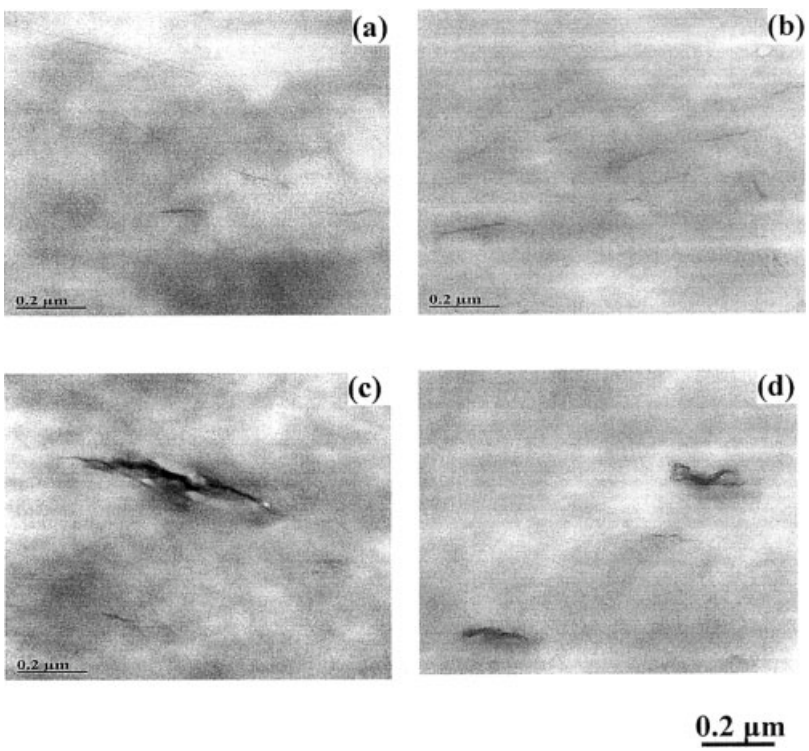

Figure 2 TEMs for LDPE/clay nanocomposites (a) WC0.05, (b) WC0.5, (c) NC0.05, (d) NC0.5.

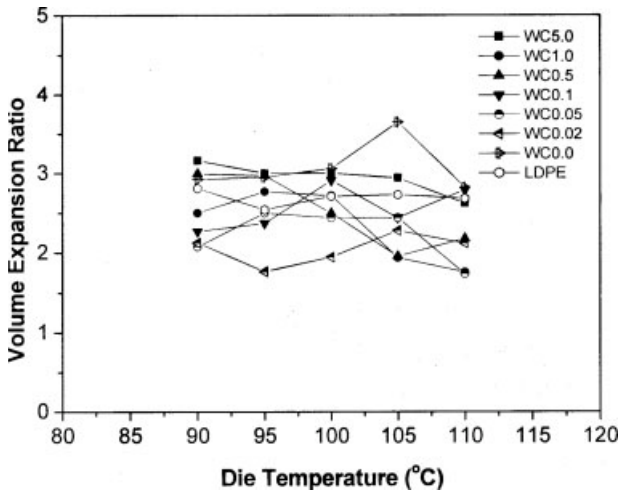

Figure 3 Effect of clay content on the volume expansion ratio of LDPE and LDPE nanocomposites.

dispersion mechanicsm proposed by Dennis et al.,[28] when the clay is melt-blended into a polymer, the primary clay particles (or aggregates) are first fractured by mechanical shear in the extruder. The polymer chains then diffuse into the clay galleries because of either a physical or chemical affinity between the polymer and the organoclay surface and push the platelets apart. After this, an onion-like delaminating process continues to disperse the platelets into the polymer matrix. The diffusion of polymer into the clay galleries is facilitated by increased residence time in the extruder, therefore potentially processing could be optimized to ensure exfoliation in the case of the LDPE/clay nanocomposites. LDPE-based nanocomposites without coupling agent exhibited one diffraction peak at a lower angle than that of pure clay, having smaller intensity. The presence of stacked silicate layers in the TEM images corroborates this finding and suggests the presence of intercalated structures.

Effects of clay content on cell morphology

Figures 3 and 4 shows the volume expansion ratio and the cell density of LDPE and LDPE/clay nanocomposite foams at processing temperatures ranging from 90°C to 110°C for different clay contents. For reference purposes, the cell densities for the blend of LDPE and PE-g-MAn (weight ratio of LDPE/PE-g-MAn = 85/15, WC0.0), as well as pure LDPE, were also included. Although no distinct difference of the volume expansion ratio was observed with an increased clay content, the cell density increased significantly by adding only small clay amounts of 0.02 wt % and 0.05 wt %. Very high cell densities ($> 10^9$ cells/cm^3) were achieved along the entire processing temperature range in the case of nanocomposites filled with 0.02–0.1 wt % clay, as shown in Figure 4(a), whereas a reduction is seen at higher loadings. Figure 4(b) shows the average cell density of each sample along an entire processing temperature for each clay content. It seems therefore that there is a strong dependence between cell density and clay content, and that an optimum content exists for maximizing the cell density. The increase in the cell density may be attributed to exfoliated clay particles acting as a nucleating agent for heterogeneous nucleation.[29–31] As clay content increased further however, the degree of exfoliation may have decreased, as evidenced by the reemergence of peaks in the XRD traces. The LDPE nanocomposite filled with 5 wt % clay, which had an intercalated structure, exhibited no pronounced effect of clay on cell nucleation. In intercalated nanocomposites most clay exists in layered stacks, therefore there is less actual

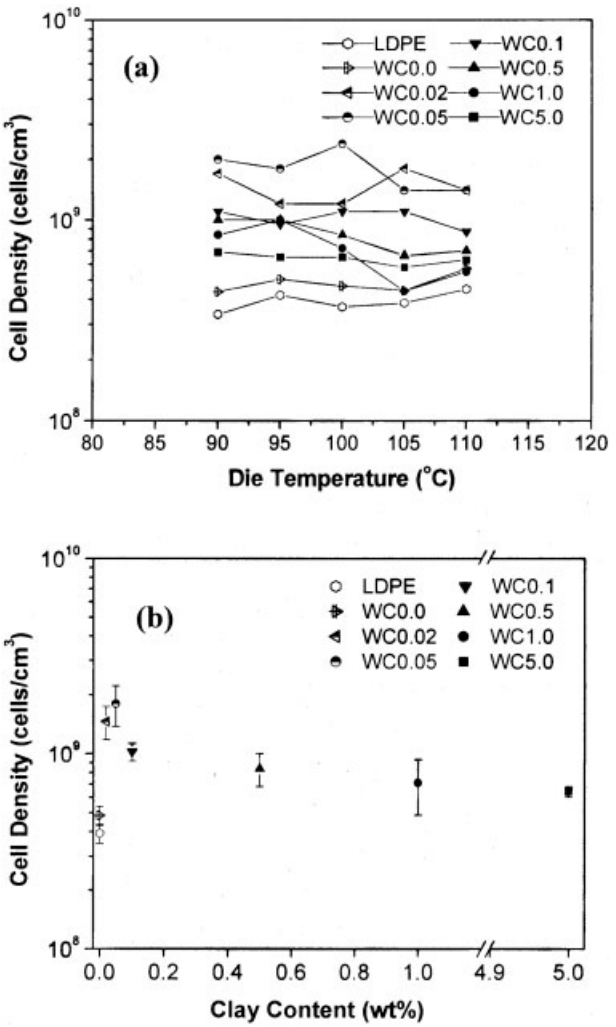

Figure 4 Effect of clay content on the cell population density of LDPE and LDPE nanocomposites with different (a) die temperature, and (b) clay content.

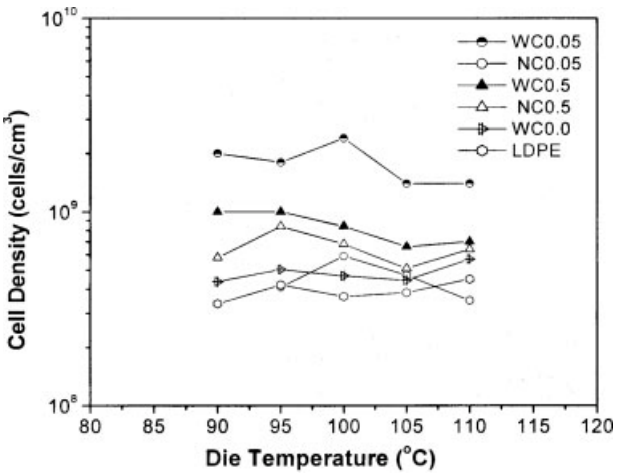

Figure 5 Effect of clay dispersion on the cell population density of LDPE and LDPE nanocomposites.

polymer-clay interfacial contact area. A completely exfoliated structure ensures maximum polymer-clay interfacial contact, thus providing more heterogeneous nucleation sites, even at very low clay contents. At this point it is not clear if the cell density would increase at higher clay loadings if higher degrees of exfoliation could be achieved.

Effect of clay dispersion on cell morphology

To study further the effect of clay dispersion in the polymer matrix on cell density, two exfoliated (WC0.05 and WC0.5) and two intercalated LDPE nanocomposites (NC0.05 and NC0.5), with clay amounts of 0.05 and 0.5 wt %, respectively, were selected. Figure 5 shows that the cell densities of WC0.05 and WC0.5 are higher than those of NC0.05 and NC0.50, implying that the exfoliated clay greatly improved the cell density in the nanocomposites. In particular, it is very interesting that a significant difference between the cell densities of the exfoliated and intercalated nanocomposites was observed at very low clay loading, 0.05 wt %. As explained above, this may be due to more polymer-clay interfacial contact area in the exfoliated nanocomposites, resulting in increased probability for heterogeneous nucleation. We also speculate that the exfoliated nanocomposites may result in a smaller activation energy for all nucleation and may inhibit the deterioration of nucleated bubbles, by acting as barriers for cell coalescence. Exfoliated nanocomposites have higher melt viscosity and stiffness,[19] thereby preventing cell coalescence even further. This would result in a smaller cell size and a higher cell density in exfoliated nanocomposites, compared with intercalated. This can be demonstrated in Figure 6, which shows that at 0.05 wt % clay the average cell size decreased from 25 μm in the case of intercalated nanocomposites to 5 μm when an exfoliated nanocomposite was generated [Fig. 6(c,d)]. At 0.5 wt % clay the average cell size decreased approximately from 15 μm to 10 μm [Fig. 6(e,f)]. Further research is needed to verify these findings.

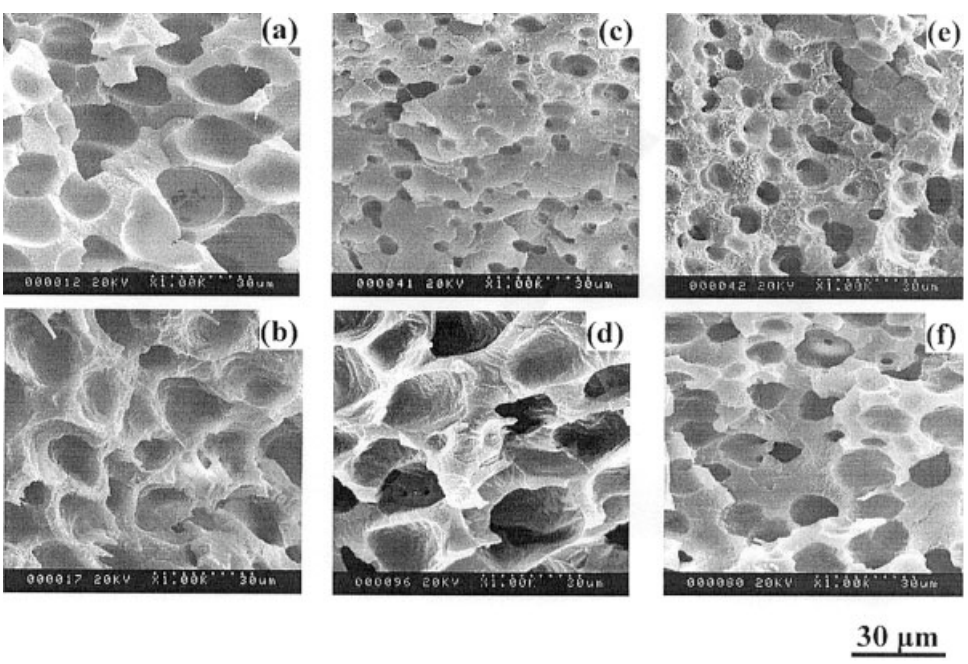

Figure 6 SEMs of (a) LDPE, (b) WC0.0, and various LDPE nanocomposites (c) WC0.05, (d) NC0.05, (e) WC0.5, (f) NC0.5 at die temperature 95°C.

CONCLUSIONS

In this study, intercalated and exfoliated LDPE/clay nanocomposites were prepared by melt blending with and without the aid of a maleated polyethylene as a coupling agent. When a small amount (< 0.1 wt %) of clay was added into LDPE with PE-g-MAn, the cell density was improved significantly (> 10^9 cells/cm^3). The optimum content of clay was 0.02–0.1 wt %, which corresponds to an extremely high cell density. However, above a critical content of 0.05 wt % clay, a decrease in cell density occurred, and no distinct effect of clay was observed in terms of cell density for the LDPE nanocomposite filled with 5 wt % clay, which showed an intercalated structure.

In consequence, it was demonstrated that achieving a higher degree of exfoliation for nanoclays is key for enhancing the cell density, even when small amounts of clay (only < 1.0 wt %) are used in the nanocomposites.

The authors express our thanks to DuPont Canada and Nova Chemicals for supplying materials. We also thank Ingenia Polymers for their help with compounding.

References

1. Martini, J.; Waldman, F. A.; Suh, N. P. SPE ANTEC Tech Pap 1982, 28, 674.
2. Baldwin, D. F.; Suh, N. P. SPE ANTEC Tech Pap 1992, 38, 1503.
3. Collias, D. I.; Baird, D. G.; Borggreve, R. J. M. Polymer 1994, 25, 3978.
4. Collias, D. I.; Baird, D. G. Polym Eng Sci 1995, 35, 1167.
5. Park, C. B.; Suh, N. P. Polym Eng Sci 1996, 36, 34.
6. Doroudiani, S.; Park, C. B.; Kortschot, M. T. Polym Eng Sci 1996, 36, 2645.
7. Doroudiani, S.; Park, C. B.; Kortschot, M. T. Polym Eng Sci 1998, 38, 1205.
8. Naguib, H. E.; Park, C. B.; Panzer, U.; Reichelt, N. Polym Eng Sci 2002, 42, 4181.
9. Park, C. B.; Lee, P. C.; Wang, J.; Valentina, P. Presented at the Polymer Processing Society (PPS) 2003 Conference, Athens, Greece, 2003; p 247.
10. Lee, M.; Tzoganakis, C.; Park, C. B. Polym Eng Sci 1998, 38, 1112–1120.
11. Park, C. B.; Baldwin, D. F.; Suh, N. P. Polym Eng Sci 1995, 35, 432–440.
12. Lee, C.; Sheth, S. H.; Kim, R. Polym Eng Sci 2001, 41, 990.
13. Ramesh, N. S.; Rasmussen, D. H.; Campbell, G. A. Polym Eng Sci 2001, 34, 1685.
14. Ramesh, N. S.; Rasmussen, D. H.; Campbell, G. A. Polym Eng Sci 2001, 34, 1698.
15. Giannelis, E. P. Adv Mater 1996, 8, 29.
16. Giannelis, E. P.; Krishnamoorti, R.; Manias, E. Adv Polym Sci 1995, 33, 1047.
17. Krishnamoorti, E.; Vaia, R. A.; Giannelis, E. P. Chem Mater 1996, 8, 1718.
18. Kojima, Y.; Usuki, A.; Kawasumi, M.; Okada, A.; Fukushima, Y.; Kurauchi, T.; Kamigaito, O. J Mater Res 1993, 8, 1185.
19. Gopakumar, T. G.; Lee, J. A.; Kontopoulou, M.; Parent, J. S. Polymer 2002, 43, 5483.
20. Wang, K. H.; Chung I. J.; Jang, M. C.; Keum, J. K.; Song, H. H. Macromolecules 2002, 35, 5529.
21. Wang, K. H.; Xu, M.; Choi, Y. S.; Chung, I. J. Polym Bull 2001, 46, 499.
22. Han, X.; Zeng, C.; Lee, L. J.; Tomasko, D. L.; Koelling, K. W. Polymer Processing Society (PPS)-18, 2002, PO23.
23. Han, X.; Zeng, C.; Lee, L. J.; Tomasko, D. L.; Koelling, K. W. SPE ANTEC Tech Pap 2002, 1915.
24. Wingert, M. J.; Han, X.; Zeng, C.; Li, H.; Lee, L. J.; Tomasko, D. L.; Koelling, K. W. SPE ANTEC Tech Pap 2003, 986.
25. Nam, P. H.; Maiti, P.; Okamoto, M.; Kotaka, T.; Nakayama, T.; Takada, M.; Ohshima, M.; Usuki, A.; Hasegawa, N.; Okamoto, H. Polym Eng Sci 2002, 42, 1907.
26. Fujimoto, Y.; Ray, S. S.; Okamoto, M.; Ogami, A.; Yamada, K.; Ueda K. Macromol Rapid Commun 2003, 24, 457.
27. Yuan, M.; Turng, L. S.; Spindler, R.; Caulfield, D.; Hunt, C. SPE ANTEC Tech Pap 2003, 691.
28. Dennis, H. R.; Hunter, D. L.; Chang, D.; Kim, S.; White, J. L.; Cho, J. W.; Paul, D. R. Polymer 2001, 42, 9513.
29. Colton, J. S.; Suh, N. P. Polym Eng Sci 1987, 27, 485.
30. Colton, J. S.; Suh, N. P. Polym Eng Sci 1987, 27, 493.
31. Colton, J. S.; Suh, N. P. Polym Eng Sci 1987, 27, 500.